



PERGAMON

International Journal of Solids and Structures 37 (2000) 1361–1383

INTERNATIONAL JOURNAL OF
**SOLIDS and
STRUCTURES**

www.elsevier.com/locate/ijsolstr

The transient dynamics of a cable-mass system due to the motion of an attached accelerating mass

Yi-Ming Wang

Division of Automobile Technology, Department and Graduate Institute of Industrial Education, College of Technology, National Chunghua Normal University, Chunghua, Taiwan

Received 11 June 1998; received in revised form 25 September 1998

Abstract

The objective of this paper is an analytical and numerical study of the transient vibrations of a taut inclined cable with a riding accelerating mass that is suspended in space. The moving mass is accelerated by a thrust down the inclined cable and is able to be aerodynamically brought to a halt. The thrust is a follow force that is tangential to the deformed configuration of the cable.

The cable is suspended from two points of different elevation. The higher point of the cable is anchored to the ground, and the lower point of the cable is controlled so that its tension at that point is held at a constant level. Hence, the length of the cable is not fixed and is a parameter to be determined during any run. The restriction in which an inextensible cannot vibrate in the limit of vanishing sag then is removed.

The mechanics of the problem is Newtonian. Methods of analysis will consist of the dynamics of small deformations superimposed on the static catenary state. The problem is nonlinear due to the presence of friction and the convective acceleration interaction of the moving mass and the cable. Galerkin's procedure for removal of spatial dependence and numerical integration are used to obtain convergent solutions. © 1999 Elsevier Science Ltd. All rights reserved.

1. Introduction

Vibrations of cables with and without moving mass have been the subject of many studies. Smith (1964) outlined analytical works to investigate the dynamic behavior of a stretched string carrying a moving mass that travels with constant velocity along the string. Analytical solutions for the vibrations of a stretched string due to moving load are carried out but the interaction of string and mass is not considered in his analysis.

Forrestal et al. (1975) considered a rocket-propelled trolley which is forced at constant acceleration along a steel cable suspended between two mountain peaks. They developed a simple model that neglects the interaction of cable and attached mass to predict deflection profile of the cable and kink angle in the cable during motion.

0020-7683/00/\$ - see front matter © 1999 Elsevier Science Ltd. All rights reserved.

PII: S0020-7683(98)00293-5

In a latter study, Rodeman et al. (1976) analyzed the dynamic response of an infinitely long ideal cable due to the motion of the attached mass. Their results show that the dynamics of the system can be significantly affected by the inertia of the moving mass.

Triantafyllou (1984) studied the mechanics of a taut inclined cable due to external forces. He points out that the effect of elasticity is particularly important in taut cables. His results indicate that an inextensible cable in the limit of vanishing sag is not possible.

Wu and Chen (1989) analyzed the dynamic response of an extensible cable suspended from two points of equal elevation due to the motion of the attached mass. They use Newmark direct integration method and the Newton–Raphson iteration approach to predict the influence of various parameters on the response of the system.

Ting et al. (1974) consider the effect of convective acceleration. The interaction between the moving mass and the supporting structure was involved. They point out that the convective acceleration terms that were not previously recognized should be included if ‘correct’ formulation is desired.

Wang (1993) analyzed the transient vibrations of an inextensible cable with a riding accelerating mass. A new model that includes the effect of rolling friction between the moving mass and the cable was developed. An important feature to be carried out is the ability to bring the mass to a halt at the end point of the cable.

In this study, the purpose is to present an analytical methodology to evaluate the transient dynamics of the motion of a cable-mass system with finite span and the influence of various parameters upon the performance of the cable.

The moving mass may be parked on the cable and may slide down the cable under a variety of conditions that include free fall under gravity and being propelled with forward/reverse forces. Rapid deceleration and braking to a halt at the desired (end) point on the cable is considered. The effect of rolling friction between the rollers of the mass and the cable is a parameter that is included in modeling of the system.

The force applied on the mass is specified and this results in variable velocity and acceleration, unknown location of the mass along the cable, nonlinear boundary and initial value problem. The problem of specification of forward and retarding forces that will cause the moving mass to acquire a specified speed and thereafter reduce speed to a halt at the desired (end) point is solved.

2. Basic formulae

In this study, an inclined taut inextensible cable suspended from two points L apart and having a difference in elevation of h is considered. The Cartesian position vector of point s along the cable at time t is represented by $\mathbf{r}(s,t)$ or is given as (Fig. 1)

$$\mathbf{r}(s,t) = x(s,t)\mathbf{i} + y(s,t)\mathbf{j} \quad (1)$$

The equations of motion then can be written as

$$(T\mathbf{r}')' + \mathbf{f} = m\ddot{\mathbf{r}}, \quad 0 < s < \ell, \quad t > 0 \quad (2)$$

with the inextensibility constraint

$$\mathbf{r}' \cdot \mathbf{r}' = 1 \quad (3)$$

where superposed prime and dot denote s and t differentiation and where T and m indicate the tension and the mass per unit length of the cable respectively. The external forces, are collectively denoted by \mathbf{f} ,

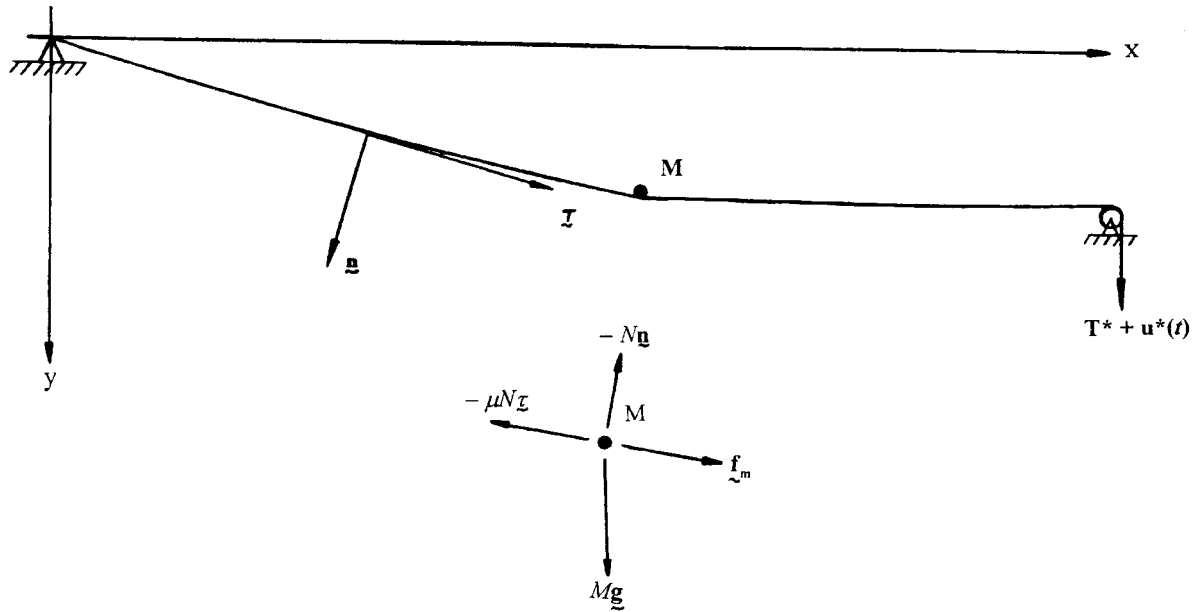


Fig. 1. Schematic of cable and the moving mass.

include the weight of the cable and the mass as well as the moving reaction of the mass upon the cable. The equation of motion of the mass, considered separately, states (Fig. 1)

$$M\mathbf{a}_m = M\mathbf{g} + \mathbf{f}_m - \mu N\boldsymbol{\tau} - N\mathbf{n} \tag{4}$$

where M = mass of the moving mass; $\mathbf{g} = g\mathbf{j}$ = acceleration of gravity; $\mathbf{f}_m = \text{thrust} = Mf\boldsymbol{\tau}$; N = reaction of cable on the mass; μ = coefficient of friction; $\boldsymbol{\tau} = \partial x/\partial s\mathbf{i} + \partial y/\partial s\mathbf{j} = \cos\theta\mathbf{i} + \sin\theta\mathbf{j}$; $\mathbf{n} = -\partial y/\partial s\mathbf{i} + \partial x/\partial s\mathbf{j} = -\sin\theta\mathbf{i} + \cos\theta\mathbf{j}$ and θ stands for the angle between $\boldsymbol{\tau}$ and the x axis.

The acceleration of the mass, \mathbf{a}_M , is obtained from

$$\mathbf{a}_M = \frac{d^2}{dt^2}[\mathbf{r}(\bar{s}(t), t)] = \mathbf{r}''(\dot{\bar{s}})^2 + 2\dot{\bar{s}}\ddot{\bar{s}} + \mathbf{r}'\ddot{\bar{s}} + \ddot{\mathbf{r}} \tag{5}$$

where $\bar{s}(t)$ is the distance along the arc of the cable designating the position of the moving mass. The force \mathbf{f} on the cable can be stated also by

$$\mathbf{f} = m\mathbf{g} + (N\mathbf{n} + \mu N\boldsymbol{\tau})\delta(s - \bar{s}) \tag{6}$$

where $\delta(s - \bar{s})$ is the Dirac delta function.

Thus the equation governing the motion of the combined system (mass and cable) becomes

$$(T\mathbf{r}')' + m\mathbf{g} + (M\mathbf{g} + \mathbf{f}_m)\delta(s - \bar{s}) = m\ddot{\mathbf{r}} + M\delta(s - \bar{s})\left[\mathbf{r}''(\dot{\bar{s}})^2 + 2\dot{\bar{s}}\ddot{\bar{s}} + \mathbf{r}'\ddot{\bar{s}} + \ddot{\mathbf{r}}\right] \tag{7}$$

while the mass obeys

$$M\left[\mathbf{r}''(\dot{\bar{s}})^2 + 2\dot{\bar{s}}\ddot{\bar{s}} + \mathbf{r}'\ddot{\bar{s}} + \ddot{\mathbf{r}}\right] = \mathbf{f}_m + M\mathbf{g} - [N\mathbf{n} + \mu N\boldsymbol{\tau}], \quad s = \bar{s}(t) \tag{8}$$

Equations (3), (7) and (8) account for \mathbf{r} , T , N and \bar{s} when m , M , μ , \mathbf{g} and the points of anchor of cable

are specified. The boundary conditions of the problem when control is being implemented (Fig. 1) are

$$\mathbf{r} = 0, \quad \text{at } s = 0 \quad (9)$$

$$\mathbf{r} = L\mathbf{i} + h\mathbf{j}, \quad \text{at } s = \ell(t) \quad (10)$$

$$T = T^* + u^*(t), \quad \text{at } s = \ell(t) \quad (11)$$

where $u^*(t)$ is the control force specified by a control algorithm and $\ell(t)$ is the total cable length to be determined.

To determine the static shape of the cable when the mass is on the cable, we define the static problem as

$$\frac{d}{ds} \left(T_0 \frac{d\mathbf{r}_0}{ds} \right) = -[m + M\delta(s - \bar{s})]\mathbf{g} \quad (12)$$

$$\frac{d\mathbf{r}_0}{ds} \cdot \frac{d\mathbf{r}_0}{ds} = 1 \quad (13)$$

with the boundary conditions

$$\mathbf{r}_0 = \mathbf{0}, \quad \text{at } s = 0 \quad (14)$$

$$\mathbf{r}_0 = L\mathbf{i} + h\mathbf{j}, \quad \text{at } s = \ell_0 \quad (15)$$

$$T_0(\ell_0) = T^* \quad (16)$$

In scalar terms eqn (12) implies

$$\frac{d}{ds} \left(T_0 \frac{dx_0}{ds} \right) = 0 \quad (17)$$

$$\frac{d}{ds} \left(T_0 \frac{dy_0}{ds} \right) = -mg - Mg\delta(s - \bar{s}) \quad (18)$$

The solution of eqn (18) satisfying eqn (13) is

$$\frac{dy_0}{dx_0} = -\sinh \beta(x_0 - c_1), \quad 0 < x_0 < \bar{x}_0 \quad (19a)$$

$$\frac{dy_0}{dx_0} = -\sinh \left[\beta(x_0 - \hat{c}_1) + \frac{Mg}{T_0(\bar{s})} \right], \quad \bar{x}_0 < x_0 < L \quad (19b)$$

where $\beta = mg/H_0$ and $H_0 = T_0 dx_0/ds =$ the horizontal component of the tension in the cable. Here, the term $Mg/T_0(s)$ in eqn (19b) can be obtained approximately by the integration of eqn (12) from $\bar{s} - \varepsilon$ to $\bar{s} + \varepsilon$ with ε denoting the small deviation of the position from the mass. A single integration of the static form of eqn (12) yields

$$T_0 \tau_0 \Big|_{\bar{s}-\varepsilon}^{\bar{s}+\varepsilon} = -Mg \tag{20}$$

In scalar terms eqn (20) implies

$$T_0 \frac{dx_0}{ds} \Big|_{\bar{s}-\varepsilon} = T_0 \frac{dx_0}{ds} \Big|_{\bar{s}+\varepsilon} = H_0 \tag{21a}$$

$$\frac{dy_0}{dx_0} \Big|_{\bar{s}+\varepsilon} - \frac{dy_0}{dx_0} \Big|_{\bar{s}-\varepsilon} = -\frac{Mg}{H_0} \tag{21b}$$

Substitution of eqns (19a) and (19b) into eqn (21b) yields

$$\frac{Mg}{T_0(\bar{s})} = -\beta(\bar{x}_0 - \hat{c}_1) + \sinh^{-1} \left[\sinh \beta(\bar{x}_0 - c_1) + \frac{Mg}{H_0} \right] \tag{22}$$

The static deflection of the cable y_0 due to the weight of the cable and the mass then can be determined from eqns (19a) and (19b) which yields

$$y_0 = \frac{1}{\beta} \left[-\cosh \beta(x_0 - c_1) + c_2 \right], \quad 0 < x_0 < \bar{x}_0 \tag{23a}$$

$$y_0 = \frac{1}{\beta} \left\{ -\cosh \left[\beta(x_0 - \bar{x}_0) + \sinh^{-1} \left[\sinh \beta(\bar{x}_0 - c_1) + \frac{Mg}{H_0} \right] \right] + \hat{c}_2 \right\}, \quad \bar{x}_0 < x_0 < L \tag{23b}$$

where c_1 , c_2 and \hat{c}_2 are the integration constants and can be determined from the conditions $y_0 = 0$ at $x_0 = 0$, $y_0 = h$ at $x_0 = L$ and $y_0|_{\bar{s}-\varepsilon} = y_0|_{\bar{s}+\varepsilon}$ at $x_0 = \bar{x}_0$.

Hence, the tension T_0 in the cable is

$$T_0 = H_0 \frac{ds}{dx_0} = H_0 \cosh \beta(x_0 - c_1), \quad 0 < x_0 < \bar{x}_0 \tag{24a}$$

$$T_0 = H_0 \frac{ds}{dx_0} = H_0 \left\{ \cosh \left[\beta(x_0 - \bar{x}_0) + \sinh^{-1} \left[\sinh \beta(\bar{x}_0 - c_1) + \frac{Mg}{H_0} \right] \right] \right\}, \quad \bar{x}_0 < x_0 < L \tag{24b}$$

The cable length at a horizontal distance x_0 from the fixed end is $s(x_0)$ and can be computed from

$$s(x_0) = \int_0^{\bar{x}_0} \left[1 + \left(\frac{dy_0}{dx_0} \right)^2 \right]^{1/2} dx + \int_{\bar{x}_0}^{x_0} \left[1 + \left(\frac{dy_0}{dx_0} \right)^2 \right]^{1/2} dx \tag{25}$$

Therefore, the total length of the cable is from $\ell_0 = s(L)$ and $T^* = T_0(\ell)$. Similarly, the curvature χ_0 and the directional components dx_0/ds and dy_0/ds can also be shown and are given in Appendix A.

The static king angle in the cable at the mass ($\equiv \phi_0$) then can be derived from eqn (21b) and is given by

$$\phi_0 \cong 2 \tan^{-1} \frac{Mg}{2H_0} \tag{26}$$

With the view to determining the derivations from the static state one sets

$$\mathbf{r}(s,t) = \mathbf{r}_0(s) + \mathbf{u}(s,t) = \mathbf{r}_0(s) + u(s,t)\tau_0 + w(s,t)\mathbf{n}_0 \tag{27}$$

$$T(s,t) = T_0(s) + \Delta T(s,t) \quad (28)$$

where \mathbf{u} and ΔT represent the displacement and change in tension from the static state and τ_0 and \mathbf{n}_0 are unit tangent and normal vectors to that state. The equation of motion, eqn (7), yields

$$[\tau_0(\Delta T) + T_0\mathbf{u}' + \Delta T\mathbf{u}']' + \mathbf{f}_m\delta(s - \bar{s}) = m\frac{\partial^2\mathbf{u}}{\partial t^2} + M\mathbf{a}_M\delta(s - \bar{s}) \quad (29)$$

The inextensibility constraint (3) becomes

$$2\mathbf{r}'_0 \cdot \mathbf{u}' + \mathbf{u}' \cdot \mathbf{u}' = 0 \quad (30)$$

The boundary conditions for \mathbf{u} become $\mathbf{u} = \mathbf{0}$ at $s = 0$. For boundary conditions (10) and (11) we set $\ell = \ell_0 + \Delta\ell$ with $\Delta\ell \ll \ell_0$. Employing Taylor's expansion to eqn (10) we have

$$\mathbf{r}_0(\ell_0) + \tau_0\Delta\ell + \mathbf{u}(\ell_0) + \mathbf{u}'(\ell_0)\Delta\ell = L\mathbf{i} + h\mathbf{j} \quad (31a)$$

which reduces to

$$\tau_0\Delta\ell + \mathbf{u}(\ell_0) + \mathbf{u}'(\ell_0)\Delta\ell = 0 \quad (31b)$$

Similarly, eqn (11) reduces to

$$[T'_0(\ell_0) + \Delta T'(\ell_0)]\Delta\ell + \Delta T(\ell_0) = u^*(t) \quad (32)$$

Eliminating $\Delta\ell$ between eqns (31b) and (32) yields

$$(T'_0 + \Delta T')\mathbf{u} + (u^* - \Delta T)(\tau_0 + \mathbf{u}') = \mathbf{0}, \quad \text{at } s = \ell_0 \quad (33)$$

In the following, we assume that \mathbf{u} and ΔT are small so that only linear terms in \mathbf{u} and ΔT are significant. Therefore, to summarize the dynamic problem, eqns (29), (30) and (8), we have

$$[(\Delta T)\tau_0 + T_0\mathbf{u}']' + \mathbf{f}_m\delta(s - \bar{s}) = m\frac{\partial^2\mathbf{u}}{\partial t^2} + M\delta(s - \bar{s})\left[(\chi_0\tau_0 + \mathbf{u}'')(\dot{\bar{s}})^2 + 2\dot{\mathbf{u}}'\dot{\bar{s}} + (\tau_0 + \mathbf{u}')\ddot{\bar{s}} + \ddot{\mathbf{u}}\right], \quad (34)$$

$$0 < s < \ell_0$$

with the inextensibility condition

$$\tau_0 \cdot \mathbf{u}' = u' - \chi_0 w = 0, \quad 0 < s < \ell_0 \quad (35)$$

and

$$M\left[(\chi_0\tau_0 + \mathbf{u}'')(\dot{\bar{s}})^2 + 2\dot{\mathbf{u}}'\dot{\bar{s}} + (\tau_0 + \mathbf{u}')\ddot{\bar{s}} + \ddot{\mathbf{u}}\right] = \mathbf{f}_m + M\mathbf{g} - N\mathbf{n} - \mu N\boldsymbol{\tau}, \quad s = \bar{s}(t) \quad (36)$$

Eqns (34)–(36) provide five equations for the five unknowns u , w , N , ΔT , and $\bar{s}(t)$. The boundary conditions, in scalar terms, are

$$u(s, t) = w(s, t) = 0, \quad \text{at } s = 0 \quad (37)$$

$$T'_0 u + u^* - \Delta T = 0 \quad \text{and} \quad w = 0, \quad \text{at } s = \ell_0 \quad (38)$$

Resolving eqn (34) in directions τ_0 and \mathbf{n}_0 yields

$$\begin{aligned}
 -T_0\chi_0(\chi_0u + w') + (\Delta T)' + \mathbf{f}_m \cdot \boldsymbol{\tau}_0\delta(s - \bar{s}) &= m\ddot{u} \\
 + M\delta(s - \bar{s})\left[-\chi_0(\chi_0u + w')(\dot{\bar{s}})^2 + \ddot{\bar{s}} + \ddot{u}\right], & \quad 0 < s < \ell_0, \quad t > 0
 \end{aligned} \tag{39}$$

$$\begin{aligned}
 [T_0(\chi_0u + w')] + \chi_0(\Delta T) + \mathbf{f}_m \cdot \mathbf{n}_0\delta(s - \bar{s}) \\
 = m\ddot{w} + M\delta(s - \bar{s})\left\{\left[\chi_0 + (\chi_0u + w')'\right](\dot{\bar{s}})^2 + 2(\chi_0u + w')\dot{\bar{s}} + (\chi_0u + w')\ddot{\bar{s}} + \ddot{w}\right\}, \\
 0 < s < \ell_0, \quad t > 0
 \end{aligned} \tag{40}$$

Similarly, considering the equation of motion of the mass, eqn (36), one has

$$M\left[-\chi_0(\chi_0u + w')(\dot{\bar{s}})^2 + \ddot{\bar{s}} + \ddot{u}\right] = \left(Mg\frac{dy_0}{ds} + \mathbf{f}_m \cdot \boldsymbol{\tau}_0\right) + N(\chi_0u + w' - \mu), \quad s = \bar{s}(t), \quad t > 0 \tag{41}$$

$$\begin{aligned}
 M\left\{\left[\chi_0 + (\chi_0u + w')'\right](\dot{\bar{s}})^2 + 2(\chi_0u + w')\dot{\bar{s}} + (\chi_0u + w')\ddot{\bar{s}} + \ddot{w}\right\} &= \left(Mg\frac{dx_0}{ds} + \mathbf{f}_m \cdot \mathbf{n}_0\right) - N, \\
 s = \bar{s}(t), \quad t > 0
 \end{aligned} \tag{42}$$

If we eliminate N between these equations by substituting for it from eqn (41) into eqn (42) and neglect nonlinear terms in u and w when comparing these terms to the linear terms in u and w and then comparing the latter to the unity, after some manipulations, we obtain

$$\begin{aligned}
 \ddot{\bar{s}} - \mu\left[\chi_0 + (\chi_0u + w')'\right](\dot{\bar{s}})^2 - 2\mu(\chi_0u + w')\dot{\bar{s}} \\
 = g\left[\frac{dy_0}{ds} + (\chi_0u + w' - \mu)\frac{dx_0}{ds}\right] + \frac{1}{M}\mathbf{f}_m \cdot [\boldsymbol{\tau}_0 + (\chi_0u + w' - \mu)\mathbf{n}_0] - \ddot{u} + \mu\ddot{w}, \\
 s = \bar{s}(t), \quad t > 0
 \end{aligned} \tag{43}$$

Thus, eqns (35), (39), (40) and (43) serve to determine $u(s,t)$, $w(s,t)$, $\Delta T(s,t)$, and $\bar{s}(t)$ subject to the boundary conditions (37) and (38). The given data of the problem consist of the information related to the static state of the cable and the forces \mathbf{f}_m that acts on the mass. It is mentioned here that as evident from eqn (43) the problem is nonlinear due to convective accelerations and friction.

The force \mathbf{f}_m acting on the mass is obtained by assuming that whenever a mass is being propelled by a force along an inclined cable, the force will be along the tangent to the vibrating cable. Hence, the force \mathbf{f}_m has the form

$$\mathbf{f}_m = Mf\boldsymbol{\tau} = Mf[\boldsymbol{\tau}_0 + (\chi_0u + w')\mathbf{n}_0] \tag{44}$$

where f is a prescribed function of time. For example, f may be a positive constant for a certain interval for the mass to increase speed and a negative constant to reduce speed and to come to a halt at the end of the cable.

Similar to what was done in the static state, the dynamic kink angle in the cable at the point where the mass is located can be obtained approximately by the integration of eqn (7) from $\bar{s} - \varepsilon$ to $\bar{s} + \varepsilon$. A single integration of eqn (7) yields

$$T(s,t)\tau \Big|_{\bar{s}-\varepsilon}^{\bar{s}+\varepsilon} = -(M\mathbf{g} + M\mathbf{a}_M + \mathbf{f}_m)_{s=\bar{s}} \tag{45}$$

where \mathbf{a}_M is defined by eqn (5). Here, we substitute $T = T_0 + \Delta T$ and $\tau = \tau_0 + \mathbf{u}'$ into eqn (45) and assume that the variation of tension ΔT is continuous at $s = \bar{s}(t)$ when the mass is mounted on wheels rolling on the cable. The kink angle in dynamic state ($\equiv \phi$) then is given by

$$\phi = \phi_0 + \Delta\phi \tag{46}$$

where $\phi_0 \cong 2 \tan^{-1} Mg/2H_0$ and $\Delta\phi = 2\sin^{-1} |\mathbf{b} \cdot \mathbf{b}|^{1/2}/2$ with $\mathbf{b} = 1/\Delta T[(\mathbf{f}_m - M\mathbf{a}_M)_{s=\bar{s}} - T_0\mathbf{u}'|_{\bar{s}} + \varepsilon\bar{s} - \varepsilon]$.

3. Method of solution

We begin by representing u and w as continuous functions. Thus kinks and abrupt changes in cable configuration can only be determined approximately. Let

$$w(s,t) = \sum_{n=1}^{\infty} v_n(t) \sin \frac{n\pi s}{\ell_0} \tag{47a}$$

$$u(s,t) = \sum_{n=1}^{\infty} v_n(t) R_n(s) \tag{47b}$$

where

$$R_n(s) = \int_0^s \chi_0 \sin \frac{n\pi s}{\ell_0} ds$$

Thus the boundary conditions (37) and (38) and the constraint relation (35) are satisfied. Next, eqns (47a) and (47b) are substituted into the tangential equation of motion, eqn (39) to determine $(\Delta T)'$, i.e.

$$(\Delta T)' = \sum_{n=1}^{\infty} (T_0\chi_0 B_n v_n(t) + mR_n \ddot{v}_n(t)) + M\delta(s - \bar{s}) \left[\ddot{\bar{s}} - (\dot{\bar{s}})^2 \chi_0 \sum_{n=1}^{\infty} B_n v_n(t) + \sum_{n=1}^{\infty} R_n \ddot{v}_n(t) \right] - \mathbf{f}_m \cdot \tau_0 \delta(s - \bar{s}), \quad 0 < s < \ell_0, \quad t > 0 \tag{48}$$

where $B_n = \chi_0 R_n + (n\pi/\ell_0) \cos(n\pi s/\ell_0)$. Integration of eqn (48) yields

$$\Delta T = \sum_{n=1}^{\infty} \left\{ \left(\int_0^s T_0\chi_0 B_n ds \right) v_n(t) + m \left(\int_0^s R_n ds \right) \ddot{v}_n(t) \right\} + b_1(t), \quad 0 < s < \bar{s}, \quad t > 0 \tag{49a}$$

$$\Delta T = \sum_{n=1}^{\infty} \left\{ \left(\int_0^s T_0\chi_0 B_n ds \right) v_n(t) + m \left(\int_0^s R_n ds \right) \ddot{v}_n(t) \right\} + M \left[\ddot{\bar{s}} - (\dot{\bar{s}})^2 \chi_0(\bar{s}) \sum_{n=1}^{\infty} B_n(\bar{s}) v_n(t) + \sum_{n=1}^{\infty} R_n(\bar{s}) \ddot{v}_n(t) - f \right] + b_2(t), \quad s < s < \ell_0, \quad t > 0 \tag{49b}$$

where $b_1(t)$ and $b_2(t)$ are constants of integration. As mentioned previously, the variation of tension, ΔT , is assumed to be continuous at $s = \bar{s}(t)$. Thus, eqns (49a) and (49b) with eqn (38) imply

$$\Delta T = T'_0(\ell_0) \sum_{n=1}^{\infty} R_n(\ell_0) v_n(t) - \sum_{n=1}^{\infty} \left\{ \left(\int_s^{\ell_0} T_0 \chi_0 B_n ds \right) v_n(t) + m \left(\int_s^{\ell_0} R_n ds \right) \ddot{v}_n(t) \right\} + u^*, \quad 0 < s < \ell_0, \quad t > 0 \tag{50}$$

This result together with eqns (47a) and (47b) can now be inserted into the normal equation of motion, eqn (40), which yields

$$\begin{aligned} & \sum_{n=1}^{\infty} \left[m \left(\sin \frac{n\pi s}{\ell_0} + \chi_0 \int_s^{\ell_0} R_n ds \right) + M \sin \frac{n\pi s}{\ell_0} \delta(s - \bar{s}) \right] \ddot{v}_n \\ & + 2(\dot{\bar{s}}) M \delta(s - \bar{s}) \sum_{n=1}^{\infty} B_n \dot{v}_n + \sum_{n=1}^{\infty} \left\{ \chi_0 \int_s^{\ell_0} T_0 \chi_0 B_n ds - \chi_0 T'_0(\ell_0) R_n(\ell_0) - (T_0 B_n)' \right. \\ & \left. + M \delta(s - \bar{s}) \left[B_n \ddot{\bar{s}} + B'_n(\dot{\bar{s}})^2 - B_n f \right] \right\} v_n + M \delta(s - \bar{s}) (\dot{\bar{s}})^2 \chi_0 - \chi_0 u^* = 0, \quad 0 < s < \ell_0, \quad t > 0 \end{aligned} \tag{51}$$

The approximate solution of the cable-mass system is to be obtained by employing the Galerkin’s method. Using Galerkin’s procedure for minimizing error, we multiply eqn (51) by $\sin j\pi s/\ell_0$ and integrate eqn (51) with respect to s from zero to ℓ_0 , thus obtaining

$$\begin{aligned} & \frac{1}{2} m \ell_0 \ddot{v}_j(t) + \sum_{n=1}^{\infty} \alpha_{nj}(\bar{s}) \ddot{v}_n(t) + 2M \bar{s} \sum_{n=1}^{\infty} \beta_{nj}(\bar{s}) \dot{v}_n(t) + \sum_{n=1}^{\infty} \left\{ \gamma_{nj} + M \left[\bar{s} B_n(\bar{s}) + (\dot{\bar{s}})^2 B'_n(\bar{s}) \right. \right. \\ & \left. \left. - f B_n(\bar{s}) \right] \sin \frac{j\pi \bar{s}}{\ell_0} \right\} v_n(t) + M (\dot{\bar{s}})^2 \chi_0(\bar{s}) \sin \frac{j\pi \bar{s}}{\ell_0} = \sigma_j \mu^*, \quad j = 1, 2, 3, \dots \quad t > 0 \end{aligned} \tag{52}$$

where α_{nj} , β_{nj} , γ_{nj} and σ_j are given in Appendix B. Also, the equation of motion of mass, eqn (43), becomes

$$\begin{aligned} & \ddot{\bar{s}} - \mu \left[\chi_0(\bar{s}) + \sum_{n=1}^{\infty} B'_n(\bar{s}) v_n \right] (\dot{\bar{s}})^2 - 2\mu \left(\sum_{n=1}^{\infty} B_n(\bar{s}) \dot{v}_n \right) \dot{\bar{s}} \\ & = g \left[\frac{dy_0}{ds} \Big|_{s=\bar{s}} + \left(\sum_{n=1}^{\infty} B_n(\bar{s}) v_n - \mu \right) \frac{dx_0}{ds} \Big|_{s=\bar{s}} \right] + f - \sum_{n=1}^{\infty} R_n(\bar{s}) \ddot{v}_n + \mu \sum_{n=1}^{\infty} \sin \frac{n\pi \bar{s}}{\ell_0} \ddot{v}_n, \quad t > 0 \end{aligned} \tag{53}$$

The equations of motion of the cable-mass system in dimensionless form can be obtained by introducing the following dimensionless quantities:

$$\begin{aligned} \tau &= \left(\sqrt{\frac{H_0}{m\ell_0^2}} \right) t, \quad \varsigma = \frac{s}{\ell_0}, \quad \xi = \frac{\bar{s}}{\ell_0}, \quad \hat{M} = \frac{M}{m\ell_0}, \quad \hat{v} = \frac{v}{\ell_0}, \\ \hat{f} &= \frac{m\ell_0}{H_0} f, \quad \hat{g} = \frac{m\ell_0}{H_0} g, \quad \hat{\lambda}_0 = \chi_0 \ell_0, \quad \hat{u}^* = \frac{u^*}{H_0} \end{aligned} \tag{54}$$

Then the equations of motion, eqns (52) and (53), become, respectively,

$$\frac{1}{2} \ddot{\hat{v}}_j(\tau) + \sum_{n=1}^{\infty} \hat{\alpha}_{nj}(\xi) \ddot{\hat{v}}_n(\tau) + 2\hat{M}\dot{\xi} \sum_{n=1}^{\infty} \hat{\beta}_{nj}(\xi) \dot{\hat{v}}_n(\tau) + \sum_{n=1}^{\infty} \left\{ \hat{\gamma}_{nj} + \hat{M} \left[\ddot{\xi} \hat{B}_n(\xi) + (\dot{\xi})^2 \hat{B}'_n(\xi) - \hat{f} \hat{B}_n(\xi) \right] \right. \\ \left. \sin j\pi\xi \right\} \hat{v}_n(\tau) + \hat{M}(\dot{\xi})^2 \hat{\chi}_0(\xi) \sin j\pi\xi = \hat{\sigma}_j \hat{u}^*, \quad j = 1, 2, 3, \dots, \quad \dot{()}' = \frac{d}{d\tau}, \quad ()' = \frac{d}{d\xi}, \quad \tau > 0 \quad (55)$$

$$\ddot{\xi} - \mu \left[\hat{\chi}_0(\xi) + \sum_{n=1}^{\infty} \hat{B}'_n(\xi) \hat{v}_n \right] (\dot{\xi})^2 - 2\mu \left(\sum_{n=1}^{\infty} \hat{B}_n(\xi) \hat{v}_n \right) \dot{\xi} \\ = \hat{g} \left[\frac{dy_0}{d\xi} \Big|_{\xi=\xi} + \left(\sum_{n=1}^{\infty} \hat{B}_n(\xi) \hat{v}_n - \mu \right) \frac{dx_0}{d\xi} \Big|_{\xi=\xi} \right] + \hat{f} - \sum_{n=1}^{\infty} \hat{R}_n(\xi) \ddot{\hat{v}}_n + \mu \sum_{n=1}^{\infty} (\sin(n\pi\xi)) \ddot{\hat{v}}_n, \quad \tau > 0 \quad (56)$$

where $\hat{\alpha}_{nj}$, $\hat{\beta}_{nj}$, $\hat{\gamma}_{nj}$, $\hat{\sigma}_j$, $\hat{B}_n(\xi)$ and $\hat{R}_n(\xi)$ are defined by Appendix B.

To write the equations of motion in matrix form, we allow j and n in eqns (55) and (56) to have the range

$$j = 1, 2, 3, \dots, N$$

$$n = 1, 2, 3, \dots, N$$

and let

$$\mathbf{y} = (\hat{v}_1, \hat{v}_2, \hat{v}_3, \hat{v}_4, \dots, \hat{v}_N)^T \quad (57)$$

Then eqns (55) and (56) can be written as

$$\mathbf{M}(\xi) \ddot{\mathbf{y}} + \dot{\xi} \mathbf{N}(\xi) \dot{\mathbf{y}} + \mathbf{K}_1(\xi) \mathbf{y} + \ddot{\xi} \mathbf{K}_2(\xi) \mathbf{y} + \dot{\xi}^2 [\mathbf{K}_3(\xi) \mathbf{y} + \mathbf{k}_1(\xi)] = \mathbf{h}(\hat{u}^*) \quad (58)$$

and

$$\ddot{\xi} + p(\mathbf{y}) \dot{\xi}^2 + q(\dot{\mathbf{y}}) \dot{\xi} + \mathbf{c}^T(\xi) \ddot{\mathbf{y}} + \mathbf{d}^T(\xi) \mathbf{y} + \gamma(\xi) = 0 \quad (59)$$

respectively. The initial conditions are

$$\dot{\mathbf{y}}(0) = \mathbf{y}(0) = 0, \quad \dot{\xi}(0) = 0 \quad \text{and} \quad \xi(0) = \xi_0 \quad (60)$$

where $\xi_0 = 0$ implies the mass is not parked on the cable before the mass is set on motion. The components of the previously defined matrices, vectors and scalars in eqns (58) and (59), i.e., \mathbf{M} , \mathbf{N} , \mathbf{K}_1 , \mathbf{K}_2 , \mathbf{K}_3 , \mathbf{k}_1 , \mathbf{h} , \mathbf{c} , \mathbf{d} , p , q and γ , are given in Appendix C.

The problem of numerical simulation of the transient vibrations of the cable system carried out by numerically integrating the governing differential eqns (58) and (59) with the associated initial conditions is specified in eqn (60). To do this, we further reduce the system by introducing

$$\mathbf{z} = (\dot{\mathbf{y}}^T, \dot{\xi}, \mathbf{y}^T, \xi)^T \quad (61)$$

where \mathbf{z} is the $2N + 2$ vector with the initial condition $\mathbf{z}(0) = (0, 0, 0, \xi_0)^T$. Then eqns (58) and (59) can be reduced to

$$\bar{\mathbf{M}} \dot{\mathbf{z}} = \bar{\mathbf{N}} \mathbf{z} + \mathbf{f}^* = 0 \quad (62)$$

In eqn (62), $\bar{\mathbf{M}}$ and $\bar{\mathbf{N}}$ are the $(2N + 2) \times (2N + 2)$ matrices and \mathbf{f}^* is the $2N + 2$ vector defined by

$$\bar{\mathbf{M}} = \begin{bmatrix} \mathbf{M} & \mathbf{K}_{2y} & \dot{\zeta}\mathbf{N} & \mathbf{0} \\ \mathbf{c}^T & 1 & \mathbf{0}^T & \dot{\zeta}p \\ [\mathbf{0}] & \mathbf{0} & \mathbf{I} & \mathbf{0} \\ \mathbf{0}^T & 0 & \mathbf{0}^T & 1 \end{bmatrix}$$

$$\bar{\mathbf{N}} = \begin{bmatrix} [\mathbf{0}] & \mathbf{0} & \mathbf{K}_1 + \dot{\zeta}^2\mathbf{K}_3 & \mathbf{0} \\ \mathbf{0}^T & q & \mathbf{d}^T & \mathbf{0} \\ -\mathbf{I} & \mathbf{0} & [\mathbf{0}] & \mathbf{0} \\ \mathbf{0} & -1 & \mathbf{0}^T & 0 \end{bmatrix}$$

$$\mathbf{f}^* = [\dot{\zeta}^2\mathbf{k}_1(\zeta) - \mathbf{h}^T(u^*), \quad \gamma, \quad \mathbf{0}^T, \quad 0]^T$$

where \mathbf{I} , $[\mathbf{0}]$ and $\mathbf{0}$ are $N \times N$ unit, $N \times N$ zero and $N \times 1$ zero matrices respectively.

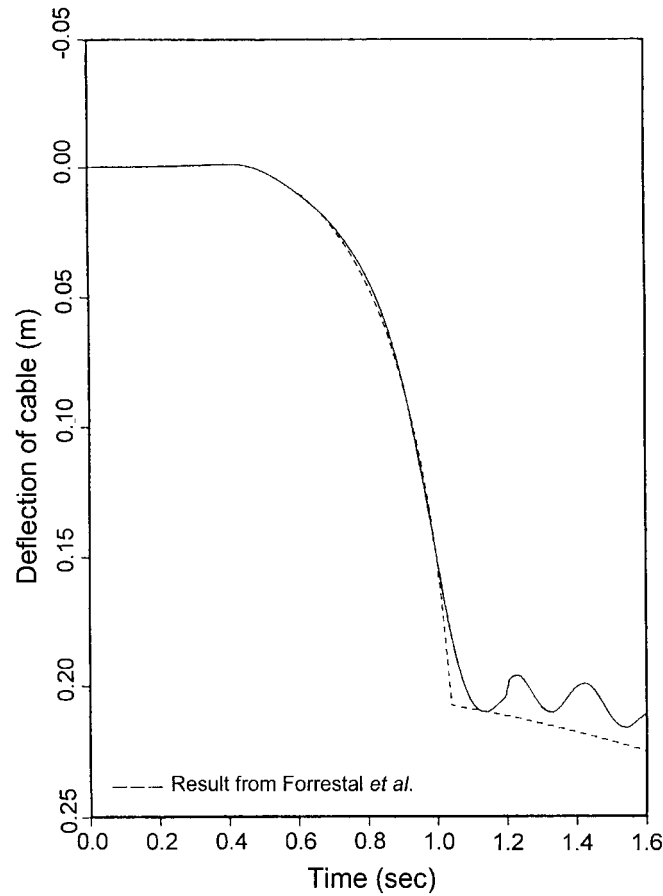


Fig. 2. A comparison between the result of this paper and the result of Forrestal et al. (1975).

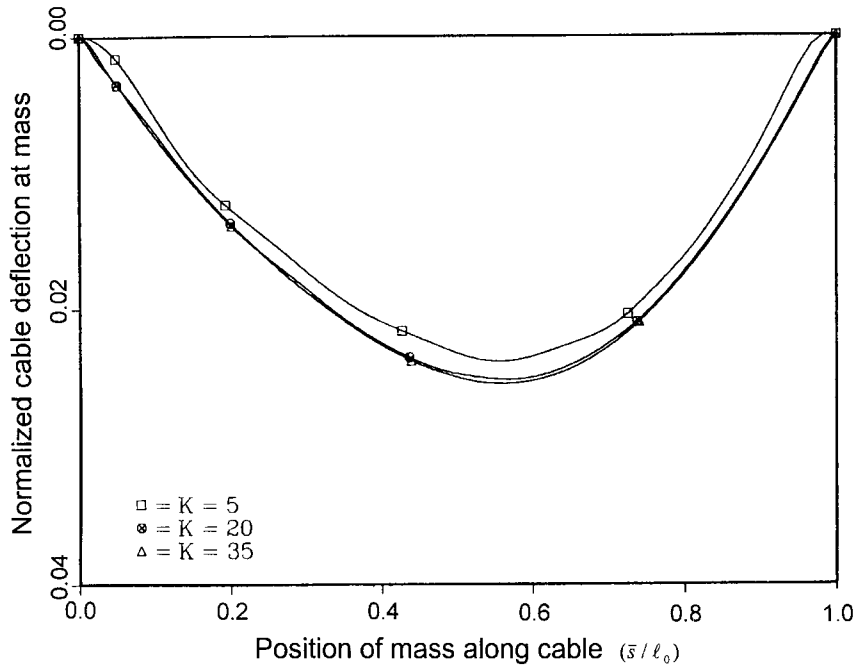


Fig. 3. Rate of convergence of solutions, with mass under free fall, with N for $H_0 = 444.8 \text{ KN}$, $\mu = 0.0$ and $Mg = 40 \text{ KN}$.

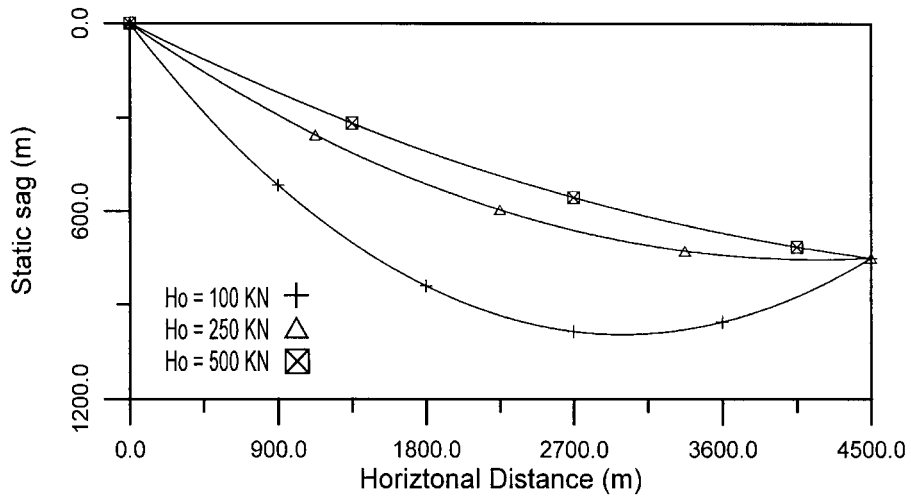


Fig. 4. Static sag of cable under its own weight vs horizontal distance for $H_0 = 100 \text{ KN}$, 250 KN and 500 KN .

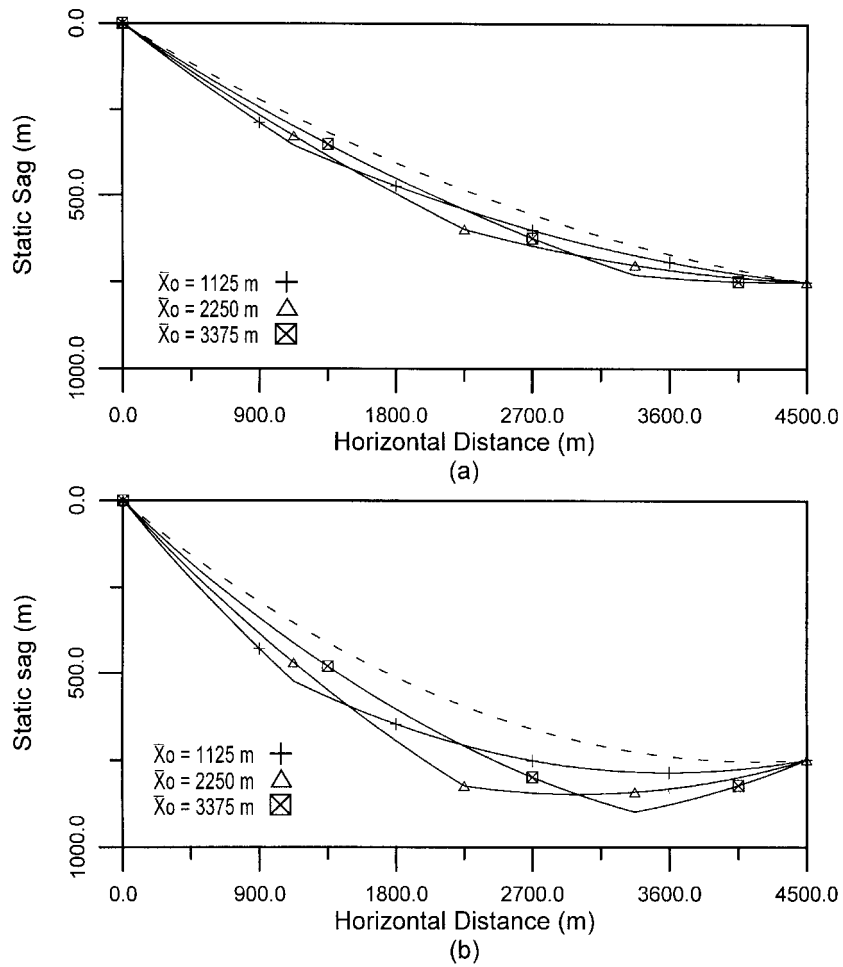


Fig. 5. Static sag of cable vs horizontal distance for $Mg = 50 \text{ KN}$, $H_0 = 250$ and 500 KN when the mass is parked at $\bar{x}_0 = 1125$, 2250 and 3375 m .

4. Numerical results and discussion

Numerical results presented here are based on the assumptions that the cable spans two mountain peaks 4500 m apart with a difference in elevation of 750 m . The material of the cable is Kevlar about 5 cm in diameter with a weight of 21.45 N m^{-1} . The weight of the mass may range up to the total weight of the cable. The mass may slide down the cable under a variety of conditions that include free fall under gravity or being propelled with thrusts. Rapid deceleration and braking to a halt at the desired (end) point are planned. The control force $u^*(t)$ is set to be zero for the work reported here.

For numerical integration of the system, eqn (62), the Runge–Kutta method with sixth order accuracy is used. Evaluation of the integrals with variable limits, such as those occurring in eqn (55), was carried out using power series technique up to $O(x^7)$. As shown in Fig. 2, the accuracy of the model was tested by comparison of its results with the results of the simpler model of Forrestal et al., (1975) which

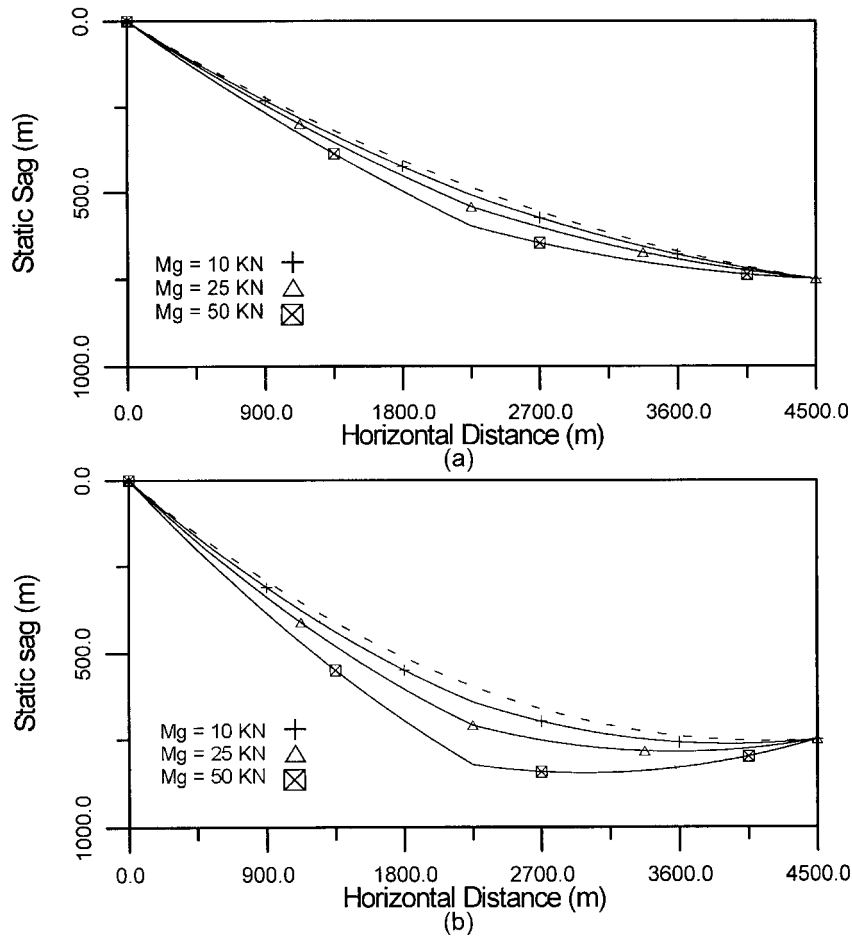


Fig. 6. Static deflection of cable with horizontal distance at $\bar{x}_0 = 2250$ m for $H_0 = 250$ kN and three values 10, 25 and 50 kN for Mg .

pertains a moving mass with constant acceleration. It is known that the latter is in agreement with experimental observations. The dimension N of \mathbf{z} in eqn (62) that was necessary to retain for sufficient accuracy was found to be 35. Fig. 3 shows the rate of convergence of cable deflection at trolley from static state, with mass under free fall, with N . There is negligible difference between the results for $N = 20$ and $N = 35$. Hence, all calculations are based on $N = 35$. The remaining parameters in Fig. 3 are $Mg = 40$ kN, $\mu = 0.0$ and $H_0 = 444.8$ kN.

In the following, an attempt is made to evaluate the influence of various parameters upon the performance of the system. The results reported below pertain to the general case when appreciable static sag, friction and variable acceleration exists.

Fig. 4 shows the static shape of the cable under its own weight for the three cases when $H_0 = 100$ kN, $H_0 = 250$ kN and $H_0 = 500$ kN. As shown in Fig. 4, the static sag in the first case, $H_0 = 100$ kN, was referred as excessive and hence the remainder of the study is carried out for the two other cases.

The results of static form of a cable with a riding mass are presented in Figs. 5–7. Fig. 5 shows the

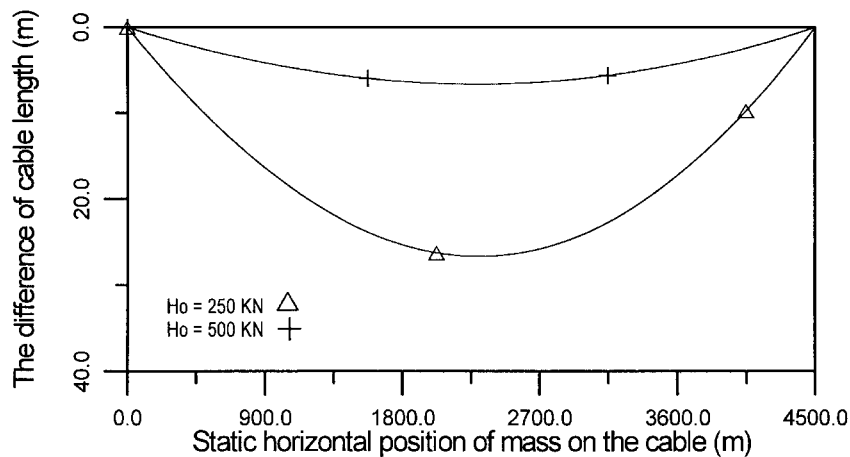


Fig. 7. The difference of cable length vs static horizontal position of mass on the cable for $Mg = 25 \text{ KN}$ and two values 250 and 500 KN for H_0 .

static deflection profile of the cable when the mass, $Mg = 50 \text{ KN}$, is parked at $\bar{x}_0 = 1125, 2250$ and 3375 m . Two different values of H_0 are selected. Fig. 5(a) is related to the case when $H_0 = 500 \text{ KN}$ and the other, Fig. 5(b), is for the condition when $H_0 = 250 \text{ KN}$. It clearly indicates that behind the mass the cable is taut and ahead of it the cable is slack. It also shows that high static tension reduces the kink angle in the cable.

Fig. 6 illustrates the static sag of the cable when the mass is parked at the midpoint of the cable ($\bar{x}_0 = 2250 \text{ m}$) for $Mg = 10, 25$ and 50 KN . The tension H_0 used in Fig. 6(a) and 6(b) are, respectively, 500 and 250 KN . The dashed lines represent the static form of the cable under its own weight. The result shows that the static sag of the cable increases with the weight of the riding mass and decreases with H_0 .

The difference of cable length with and without a riding mass under constant static tension is shown in Fig. 7. The parameters used in this figure are $Mg = 25 \text{ KN}$ and two values of static tension $H_0 = 250$ and 500 KN . This illustrates that higher tension in the cable results in lower value of the variation of cable length.

The dynamic behaviors of the system due to the motion of a riding accelerating mass are given in Figs. 8–12. As mentioned previously, the propelling force on the mass is specified and this results variable velocity, acceleration and unknown location of the mass along the cable. Therefore, the trajectory and speed of the mass on the cable are quantities of interest. Fig. 8(b) and (a), respectively, show the trajectory and velocity of the mass traveling along the cable under free fall, $f = 0.0$. The parameters used are $Mg = 25 \text{ KN}$, $\mu = 0.0$ and three values 250, 500 and 750 KN for H_0 . The result indicates that if the tension of the cable is not high enough, the speed of mass will initially increase and thereafter decrease as the mass moves to the lower point. This is expected since under low tension there exists a point of maximum sag within the two supports.

The effect of retarding force to the mass is studied in Fig. 9. In this figure, the traveling speed is plotted with the location of mass along the cable for $Mg = 25 \text{ KN}$ and two values 250 KN , Fig. 9(b), and 500 KN for H_0 under free fall. Three values of reverse force, $f = 0.0, -2.5$ and -5 m s^{-2} are

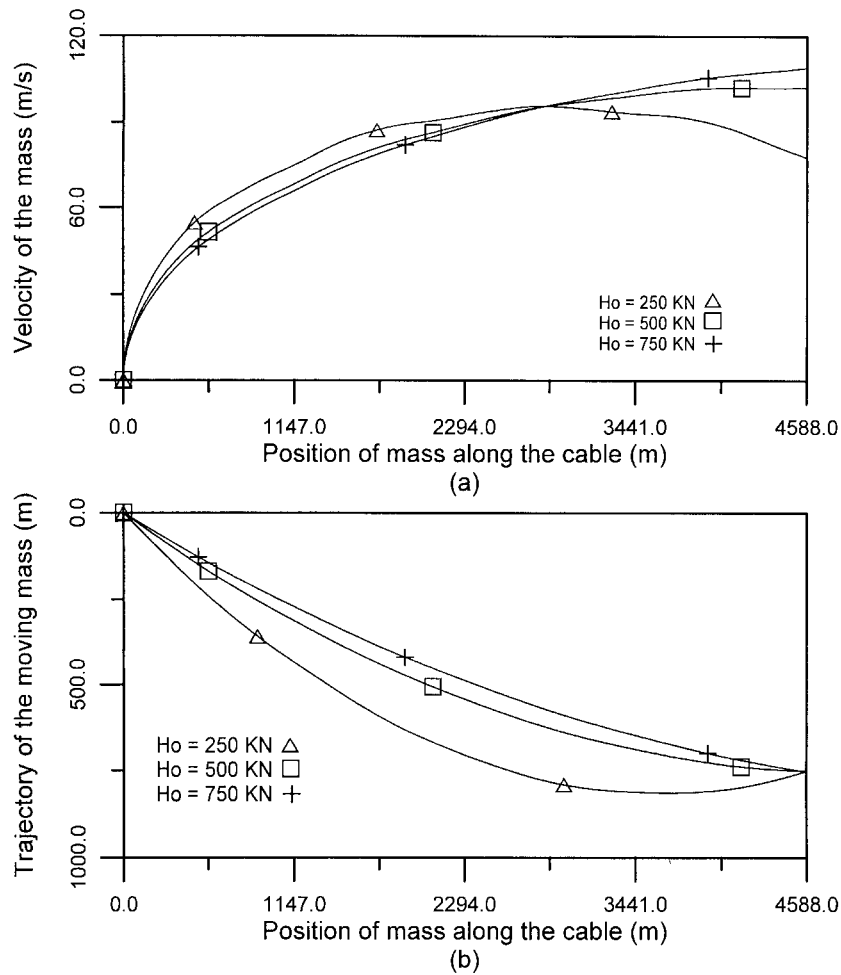


Fig. 8. The trajectory and velocity of mass vs position of mass along the cable for $Mg = 25 \text{ KN}$, $\mu = 0$ and three values 250, 500 and 750 KN for H_0 .

selected and is applied at $\bar{s}/\ell_0 = 0.6$ respectively. The result indicates that the speed of mass increases with the propelling thrust and thereafter reduces speed to a halt with the applied retarding force.

Another important operational requirement is the ability to bring the mass to a halt at the end point by a constant reverse force applied after the mass has achieved specified speed under forward thrust. The program here developed is capable of predicting the magnitude of the reverse force for any position and speed of the mass. The problem is solved by first determining the terminal velocity of the mass when forward thrust is set to zero at a particular point and then coasts to the end point. The end velocity is thus made zero by adding reverse force at that particular point and using iteration.

Fig. 10 indicates the trajectory of the mass, Fig. 10(b), and correspondingly the velocity of the mass along the trajectory under free fall. This is of the value when the location of the moving mass is of primary concern. The parameters used in this figure are $H_0 = 500 \text{ KN}$, $\mu = 0.0$ and two values 25 and 50

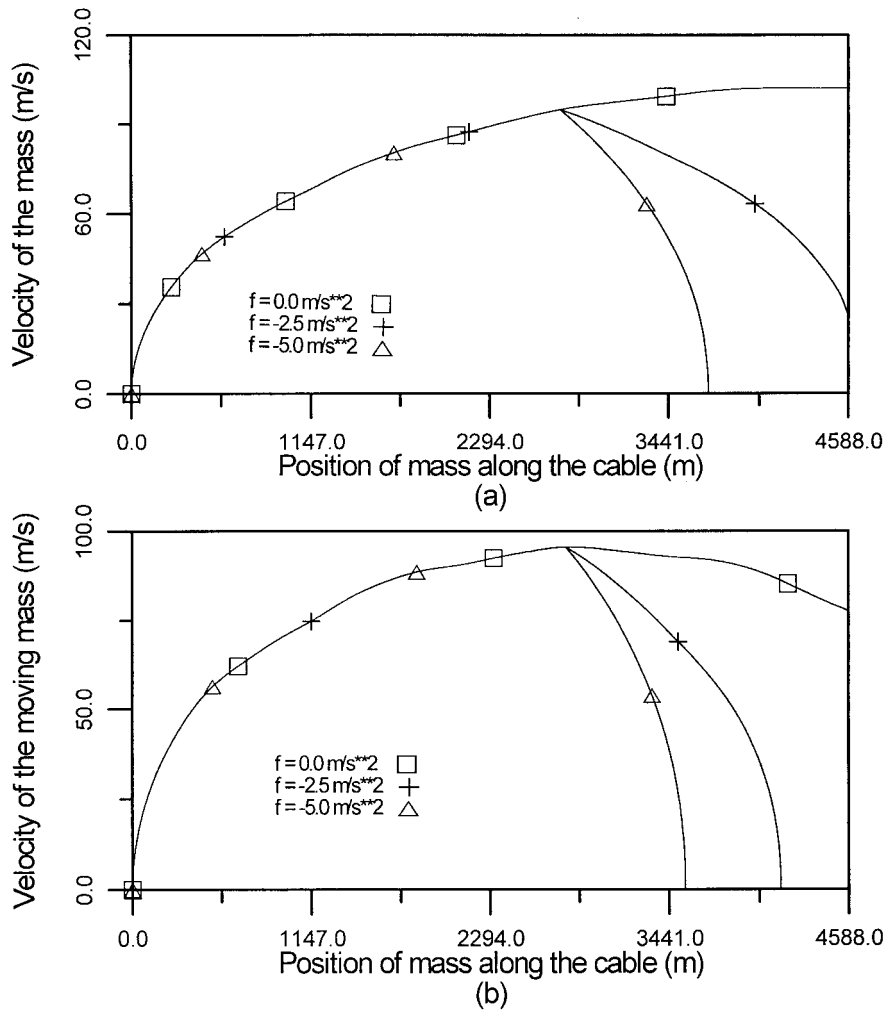


Fig. 9. The traveling speed with the position for mass along cable for $Mg = 25\text{ KN}$, $\mu = 0.0$ and two values 250 (lower plot) and 500 KN (upper plot) for H_0 under free fall. Three values of retard force $f = 0.0, -2.5$ and -5 m s^{-2} are, respectively, applied at $\bar{s}/\ell_0 = 0.6$.

KN for Mg . The retarding force is assumed to be applied at $\bar{s}/\ell_0 = 0.6$. Fig. 11 shows information to that shown in Fig. 10, except in this figure two values of the forward thrust, $f = 0.0$ and 5.0 m s^{-2} , are selected. The other parameters used are $H_0 = 500\text{ KN}$, $\mu = 0.0$ and $Mg = 25\text{ KN}$. Based on the results it appears that the speed of moving mass and the reverse force required in order to stop the mass at the end point decrease with the weight of the mass (Fig. 10). This is expected since increase in the weight of the mass will sharpen the kink angle in the cable. Meanwhile, larger values of forward thrust is applied, faster traveling speed is obtained and accordingly bigger values of reverse force for zero terminal speed are required (Fig. 11).

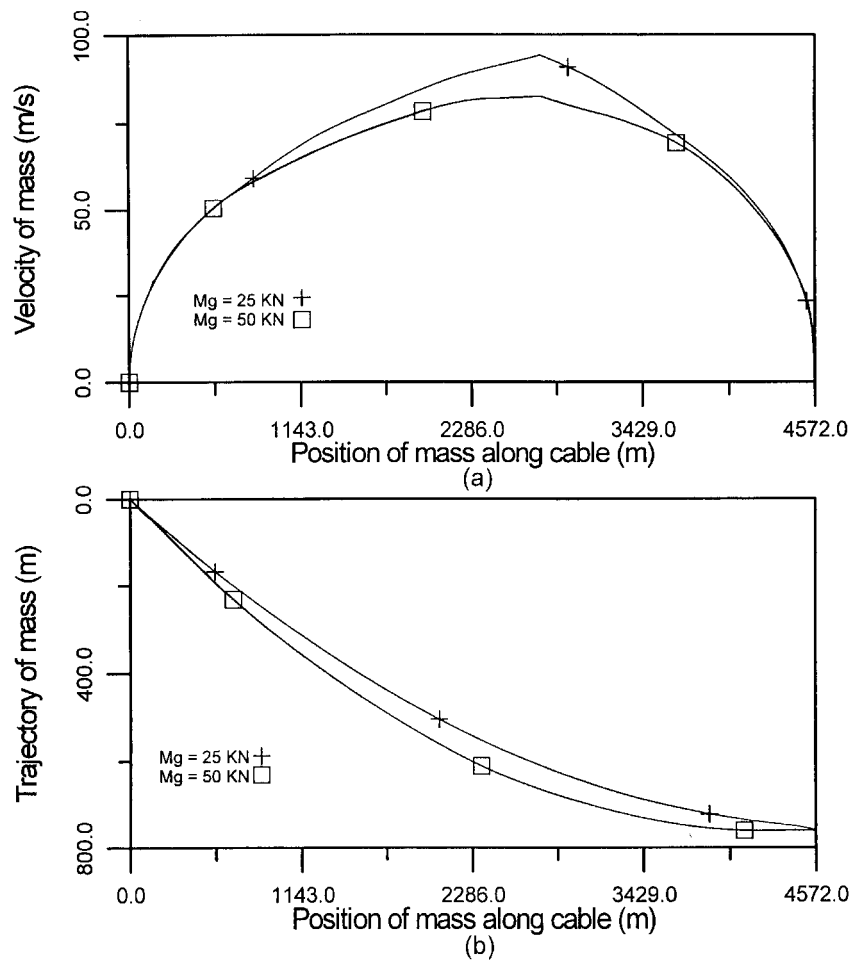


Fig. 10. Trajectory (lower plot) and velocity of the mass along the trajectory under free fall for $H_0 = 500 \text{ KN}$, $\mu = 0$ and two values 25 and 50 KN for Mg . The retard force is applied at $\bar{s}/\ell_0 = 0.6$.

Fig. 12 illustrates the value of the retarding force vs the forward thrust for zero terminal speed when assuming that the former is applied at $\bar{s}/\ell_0 = 0.6$ for $Mg = 100 \text{ KN}$, $H_0 = 500 \text{ KN}$ and two values of μ , $\mu = 0.0$ and $\mu = 0.1$. The result shows that the reverse force increases almost linearly with the forward thrust. Moreover, if the friction between the mass and the cable is not zero then the reverse force that is required to stop the mass at the end point decreases as the friction is increased.

5. Conclusions

In this study, the mechanics and transient dynamics of an inclined inextensible cable suspended from

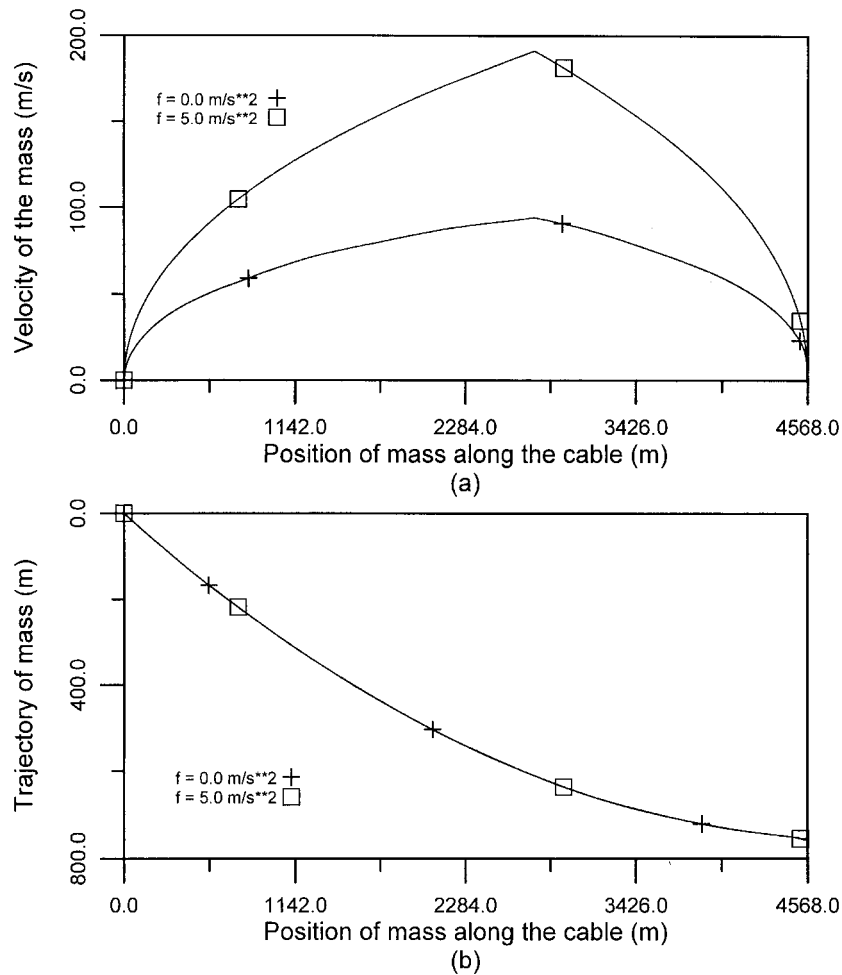


Fig. 11. Trajectory (lower plot) and velocity of the mass along the trajectory for $H_0 = 500 \text{ KN}$, $\mu = 0$, $Mg = 25 \text{ KN}$ and two values 0.0 and 5 m s^{-2} for forward thrust. The retard force is applied at $\bar{s}/\ell_0 = 0.6$.

two points of different elevation with a riding accelerating mass are studied. The restriction that an inextensible cable cannot vibrate in the limit of vanishing sag, Triantafyllou (1984), was removed by letting the length of the cable vary with the position of the mass on the cable. To accomplish this, the higher point of the cable is anchored to the ground, and the lower point of the cable is controlled so that its tension at that point is held at a constant level. Hence, the length of the cable is not fixed and is a function of the position of the moving mass during operation. This arrangement thus removes the restriction on inextensible cable under very high tension.

The mechanics of the interface between the mass and the cable are determined by modeling the mass as a rigid body that travels on a flexible structure. The interaction force, caused by convective acceleration and friction of the mass traveling on the cable is hence a function of the cable

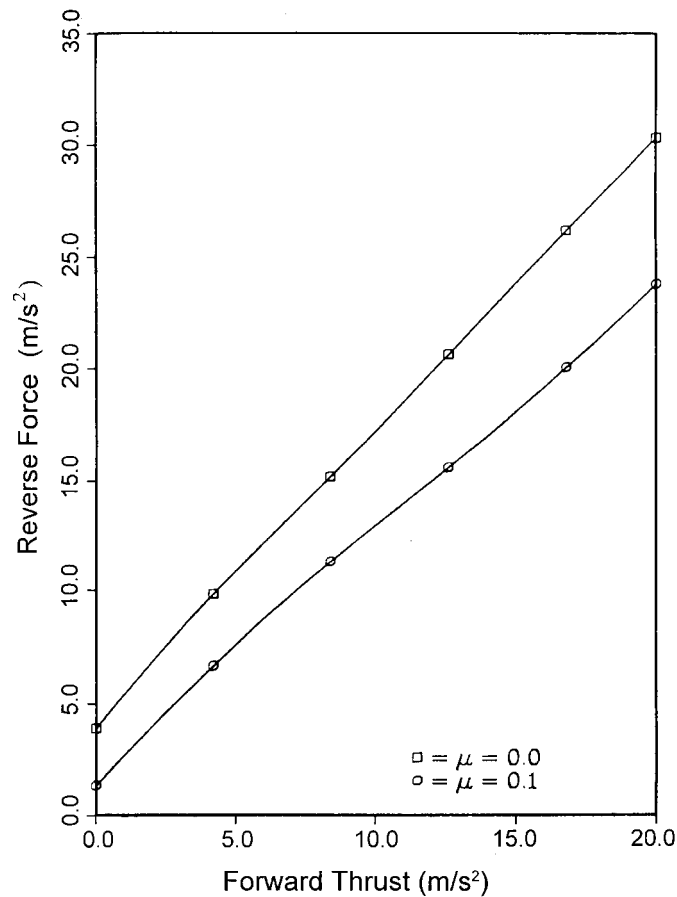


Fig. 12. Reverse force vs forward thrust for zero terminal speed when $H_0 = 500$ KN, $Mg = 100$ KN and $\mu = 0.0$ and 0.1 . The reverse thrust is applied at $\bar{s} = 0.6\ell_0$.

displacements. Therefore, there exists a nonlinear coupling between the deflection of the cable and the function that presents the position of the moving mass on the cable. Further, due to the presence of friction and convective acceleration, the problem is nonlinear. Even the differential equations of motion are obtained by superimposing small displacements on the catenary state of the cable.

Acknowledgements

Some of the original concepts of this paper were from the author's former advisor Professor Iradj G. Tadjbakhsh (1928–1993). The work reported here was supported by the National Science Council, Taiwan, under grant no. NSC87-2212-E-018-002 to National Chunghua Normal University.

Appendix A

$$\chi_0 = \frac{-\beta}{\cosh^2 \beta(x_0 - c_1)}, \quad 0 < x_0 < \bar{x}_0$$

$$\chi_0 = \frac{-\beta}{\cosh^2 \left\{ \beta(x_0 - \bar{x}_0) + \sinh^{-1} \left[\sinh \beta(x_0 - c_1) + \frac{Mg}{H_0} \right] \right\}}, \quad \bar{x}_0 < x_0 < L$$

$$\frac{dx_0}{ds} = \frac{1}{\cosh^2 \beta(x_0 - c_1)}, \quad 0 < x_0 < \bar{x}_0$$

$$\frac{dx_0}{ds} = \frac{1}{\cosh^2 \left\{ \beta(x_0 - \bar{x}_0) + \sinh^{-1} \left[\sinh \beta(x_0 - c_1) + \frac{Mg}{H_0} \right] \right\}}, \quad \bar{x}_0 < x_0 < L$$

$$\frac{dy_0}{ds} = -\tanh \beta(x_0 - c_1), \quad 0 < x_0 < \bar{x}_0$$

$$\frac{dy_0}{ds} = -\tanh \left\{ \beta(x_0 - \bar{x}_0) + \sinh^{-1} \left[\sinh \beta(x_0 - c_1) + \frac{Mg}{H_0} \right] \right\}, \quad \bar{x}_0 < x_0 < L$$

Appendix B

$$\alpha_{nj} = M \sin \frac{n\pi\bar{s}}{\ell_0} \sin \frac{j\pi\bar{s}}{\ell_0} + m \int_0^{\ell_0} \chi_0(s) \left(\int_s^{\ell_0} R_n(s) ds \right) \sin \frac{j\pi s}{\ell_0} ds$$

$$\beta_{nj} = B_n(\bar{s}) \sin \frac{j\pi\bar{s}}{\ell_0}$$

$$\gamma_{nj} = \int_0^{\ell_0} \left[\chi_0(s) \left(\int_s^{\ell_0} T_0(s) \chi_0(s) B_n(s) ds \right) \sin \frac{j\pi s}{\ell_0} \right] ds - T_0'(\ell_0) R_n(\ell_0) \int_0^{\ell_0} \chi_0(s) \sin \frac{j\pi s}{\ell_0} ds - \int_0^{\ell_0} (T_0 B_n)' \sin \frac{j\pi s}{\ell_0} ds$$

$$\sigma_j = \int_0^{\ell_0} \chi_0(s) \sin \frac{j\pi s}{\ell_0} ds$$

$$\hat{\alpha}_{nj} = \hat{M} \sin(n\pi\xi) \sin(j\pi\xi) + \int_0^1 \hat{\chi}_0(\xi) \left(\int_\xi^1 \hat{R}_n(\varsigma) d\varsigma \right) \sin(j\pi\varsigma) d\varsigma = \frac{1}{m\ell_0} \alpha_{nj}$$

$$\hat{\beta}_{nj}(\xi) = \hat{B}_n(\xi) \sin(j\pi\xi) = \ell_0 \beta_{nj}$$

$$\hat{\gamma}_{nj} = \int_0^1 \left[\hat{\chi}_0(\xi) \left(\int_{\xi}^1 \frac{d\zeta}{dx_0} \hat{\chi}_0(\zeta) \hat{B}_n(\zeta) d\zeta \right) \sin(j\pi\xi) \right]$$

$$d\xi - \left(\frac{d\xi}{dx_0} \right)' \Big|_{\xi=1} \hat{R}_n(\xi) \Big|_{\xi=1} \int_0^1 \hat{\chi}_0(\zeta) \sin(j\pi\zeta) d\zeta - \int_0^1 \left(\frac{d\xi}{dx_0} \hat{B}_n(\xi) \right)' \sin(j\pi\xi) d\xi = \frac{\ell_0}{H_0} \gamma_{nj}$$

$$\hat{\sigma}_j = \int_0^1 \hat{\chi}_0(\xi) \sin(j\pi\xi) d\xi = \sigma_j$$

$$\hat{B}_n(\xi) = \hat{\chi}_0 R_n(\xi) + n\pi \cos(n\pi\xi) = \ell_0 B_n$$

$$\hat{R}_n(\xi) = \int_0^{\xi} \hat{\chi}_0 \sin(n\pi\zeta) d\zeta = R_n(s)$$

Appendix C. components of matrices and vectors and scalar coefficients

$$M_{jn} = \frac{1}{2} \delta_{jn} + \hat{\alpha}_{jn}$$

$$N_{jn} = 2\hat{M}\hat{\beta}_{jn}$$

$$K_{1jn} = \hat{\gamma}_{jn} - \hat{M}\hat{f}\hat{B}_n \sin(j\pi\xi)$$

$$K_{2jn} = \hat{M}\hat{B}_n \sin(j\pi\xi)$$

$$K_{3jn} = \hat{M}\hat{B}'_n \sin(j\pi\xi)$$

$$K_{1j} = \hat{M}\hat{\chi}_0 \sin(j\pi\xi)$$

$$h_j = \hat{\sigma}_j \hat{u}^*$$

$$p = -\mu[\hat{\chi}_0 + (\mathbf{y}^T \mathbf{B}' \mathbf{1})]$$

$$q = -2\mu(\hat{\mathbf{y}}^T \mathbf{B}^T \mathbf{1})$$

$$\gamma = -\hat{g} \left(\frac{dy_0}{d\zeta} - \mu \frac{dx_0}{d\zeta} \right) \Big|_{\zeta=\xi} - \hat{f}$$

$$\mathbf{c}^T = \mathbf{1}^T [\mathbf{R} - \mu \mathbf{S}]$$

$$\mathbf{d}^T = - \left(\hat{g} \frac{dx_0}{d\zeta} \Big|_{\zeta=\xi} \right) \mathbf{1}^T \mathbf{B}$$

$$\mathbf{B} = \text{diag}[\hat{\mathbf{B}}_n], \quad n = 1, 2, 3, \dots, K$$

$$\mathbf{R} = \text{diag}[\hat{\mathbf{R}}_n] \quad n = 1, 2, 3, \dots, K$$

$$\mathbf{S} = \text{diag}[\sin(n\pi\xi)], \quad n = 1, 2, 3, \dots, K$$

$$\mathbf{1} = (1, 1, \dots, 1)^T, \quad K \times 1 \quad \text{unitmatrix}$$

$$[\mathbf{1}] = \mathbf{1} \mathbf{1}^T$$

References

- Alexsandradis, A.A., Dowell, E.H., Moon, E.C., 1978. The coupled response of a dynamic element riding on a continuously supported beam. *J. Applied Mech.* 45, 864–890.
- Forrestal, M.J., Bickel, D.C., Sagartz, M.J., 1975. Motion of a stretched cable with small curvature carrying an accelerating mass. *AIAA J.* 13, 1533–1535.
- Fryba, L., 1972. *Vibration of Solids and Structures Under Moving Loads*. Noordholt International Publishing, The Netherlands.
- Irvine, H.M., 1981. *Cable Structures*. MIT Press, Cambridge.
- Rodeman, R., Longcope, D.B., Shampine, L.F., 1976. Response of a string to an accelerating mass. *J. Applied Mech.* 14, 675–680.
- Sagartz, M.J., Forrestal, M.J., 1975. Motion of a stretched string loaded by an accelerating force. *J. Applied Mech.* 13, 505–506.
- Smith, C.E., 1964. Motions of a stretched string carrying a moving mass particle. *J. Applied Mech.* 31, 29–37.
- Steele, C.R., 1967. The finite beam with a moving load. *J. Applied Mech.* 34, 111–118.
- Steele, C.R., 1971. Beams and shells with moving loads. *Int. J. Solids Struct.* 7, 1171–1198.
- Ting, E.C., Genin, J., Ginsberg, J.H., 1974. A general algorithm for moving mass problems. *J. Sound and Vibrations* 33, 49–58.
- Triantafyllou, M.S., 1984. The dynamics of a taut inclined cable. *Q.J. Mech. and Applied Maths* 37, 421–440.
- Wang, Y.M., 1993. *Cable dynamics—part I: the transient vibrations of a taut inclined cable with a riding accelerating mass*. PhD thesis. Rensselaer Polytechnic Institute, Troy, New York.
- Wang, Y.M., 1998. The dynamic analysis of a finite inextensible beam with an attached accelerating mass. *Int. J. Solids Struct.* 35, 831–854.
- Wu, J.S., Chen, C.C., 1989. The dynamic analysis of a suspended cable due to a moving load. *Int. J. Numer. Method in Engrg* 28, 2361–2381.